minerals

MDPI

Article

Research on Reducing Shrinkage Behavior of Ground Granulated Blast Furnace Slag Geopolymers Using Polymer Materials

Wen-Ten Kuo *, Chuen-Ul Juang and Yu-Wei Shiu

Department of Civil Engineering, National Kaohsiung University of Science and Technology, Kaohsiung 807618, Taiwan; 1105412101@nkust.edu.tw (C.-U.J.); 1105312116@nkust.edu.tw (Y.-W.S.)
* Correspondence: wtkuo@nkust.edu.tw

Abstract: Geopolymers are a new type of environmentally friendly cement-based material with serious drying shrinkage problems. In order to overcome this problem and improve the engineering performance and durability of geopolymers, in this study we added 0%, 0.3%, 0.5%, 0.7%, and 0.9% polymer materials, namely, polyacrylamide, sodium polyacrylate, and sodium tetraborate, respectively, to geopolymers to reduce their degree of shrinkage. We also assessed changes in their length and durability to determine how the addition of polymer materials could reduce their degree of shrinkage. The results indicate that 0.7% sodium tetraborate yielded the most favored shrinkage, and, through imaging technology, the crack change at the age of 0–3 days was measured, during which polyacrylamide (PAM) effectively slowed down the dimensions of crack propagation by 0.47% compared with the control group.

Keywords: polymer materials; ground granulated blast furnace slag geopolymers; steel ring strain; shrinkage

Citation: Kuo, W.-T.; Juang, C.-U.; Shiu, Y.-W. Research on Reducing Shrinkage Behavior of Ground Granulated Blast Furnace Slag Geopolymers Using Polymer Materials. *Minerals* **2023**, *13*, 475. https://doi.org/10.3390/min13040475

Academic Editors: Fernando Pelisser and Dachamir Hotza

Received: 13 February 2023
Revised: 21 March 2023
Accepted: 25 March 2023
Published: 28 March 2023

1. Introduction

Large amounts of cement are used in civil engineering projects. Cement is manufactured by grinding and burning materials, and this manufacturing process releases large amounts of carbon dioxide. Therefore, several researchers have attempted to develop ground granulated blast furnace slag (GGBFS), which is regarded as an environmentally friendly cementitious material that can replace cement. Adding GGBFS to environmentally friendly concrete produces certain properties, such as high early strength, resistance to acidic and alkaline corrosion, resistance to high temperatures [1], and a low thermal conduction rate. Geopolymers are typically made of a large variety of raw materials. This is because they are usually composed of any mineral or waste that is rich in silicon or aluminum. Compared with normal concrete, GGBFS geopolymers perform better in civil engineering applications. Adediran et al.'s [2] study on Fe-rich fayalite-slag-based alkali-activated materials (AAMs) found that, when catalyzed at high temperatures, they experienced a more stable crystalline phase, resulting in better compressive strength [3,4]. In addition, the manufacturing process of geopolymers generates 80% less carbon dioxide than that released during the production of Portland cement. Therefore, geopolymers are currently considered the most environmentally friendly material with the potential to replace cement. In general, the use of an alkali activator to improve ash activity helps enhance the compressive strength of geopolymers. However, the setting time fluctuations, alkali–aggregate reactions, and increased volume often result in negative effects, such as specimen shrinkage and cracking. During this process, the alkali activator produces a type of paste, which undergoes a reaction similar to a pozzolanic reaction. From this, afwillite is produced as the main hydration product, which then fills in the pores and refines the internal structure. This process decreases the pore diameter, which, in turn, increases the

surface area and surface tension. Therefore, the loss of water leads to shrinkage, which reduces the intensity of development and negatively affects the durability and safety of the buildings constructed using these materials [5]. Shrinkage can be categorized into autogenous shrinkage, carbonation shrinkage, and drying shrinkage. Generally, shrinkage refers to a decrease in volume without an external load at a constant temperature. It is a phenomenon that indicates the poor volume stability of a material, which, in turn, affects its durability. Autogenous shrinkage refers to a decrease in the volume of cement during the hydration process. Carbonation shrinkage refers to a decrease in the volume of cement during the reaction between the product of cement hydration and carbon dioxide in the environment. Finally, drying shrinkage refers to a decrease in the volume of cement during the dehydration process of cement and concrete materials [6,7]. Yang et al. [8] reported that curing specimens in the presence of moisture may decrease the rate of shrinkage and prevent the development of large cracks in specimens. One inexpensive approach to reducing the rate of shrinkage and the frequency of cracking is to increase the demolding time. Using scanning electron microscopy (SEM), nuclear magnetic resonance imaging, mercury intrusion porosimetry, and thermogravimetric analysis in microscopic tests, Olawuyi et al. [9], Ma et al. [10], and Plank et al. [11] reported that superabsorbent polymers (SAPs) can effectively increase the freezing resistance and durability of geopolymers. SAPs are typically made of strong hydrophilic polymer materials, which have a high water absorption rate and water retention capacity. With the enhancement of the water release characteristics of SAPs, the curing effect of polymers considerably increases [12]. Tu et al. [13] used SAPs to slow down the cracking process of fly-ash-based geopolymers. They reported that the addition of 0%–0.5% SAPs effectively increased the workability of fresh concrete but decreased its compressive strength.

Wang et al. [14] indicated that improving the material composition and manufacturing process of geopolymers may effectively reduce the number of cracks caused by shrinkage and rapid hardening. They highlighted that the material composition can be improved through the inclusion of fillers and alkaline solutions, whereas the manufacturing process can be improved by changing the humidity of the curing environment and delaying the demolding process.

Bakharev et al. [15] reported that by adding a 6% air-entraining agent with GGBFS to cement the paste inhibited the process of autogenous and drying shrinkage. They indicated that the rates of autogenous and drying shrinkage were both lower than those of normal Portland cement because the air-entraining agent created numerous tiny bubbles within the alkaline-activated slag paste, which changed the distribution of the pores and reduced the degree of shrinkage. However, this air-entraining agent did not affect the compressive strength of the material and only slightly improved the mobility of the paste.

Palacious et al. [16] reported that the addition of a 2% shrinkage-reducing admixture (SRA) to 50-day-old GGBFS geopolymers resulted in alkali-activated GGBFS geopolymers with an autogenous shrinkage rate lower than that of normal Portland cement. However, after 50 days, the autogenous shrinkage rate of the alkali-activated slag geopolymers gradually became higher than that of the cement. These results indicated that the addition of SRA inhibited the drying shrinkage process.

Bakharev et al. [17] exposed alkali-activated slag concrete to the open air and cured it first for 2 h and then at 65 °C for 6 h. They reported that the alkali-activated slag concrete specimen exhibited less evident drying shrinkage at high temperatures than that of the specimen cured in the open air. This is because curing at a higher temperature provided more free energy, which accelerated the polymerization process and generated large amounts of afwillite, thereby reducing the generation of small pores.

Geopolymers typically undergo an exothermic dehydration reaction, which removes extra moisture and leads to shrinkage. To avoid the development of early cracks, several methods can be used to reduce autogenous shrinkage [18]. This is usually achieved by adding polymer materials with strong water absorption properties, such as sodium polyacrylate (SP), polyacrylamide (PAM), and acrylic acid. SAPs are mainly used in

hygiene and convenience products. Each SAP polymer can store up to 1500 g of water [19]. These SAPs are used in cement to absorb moisture in the cement paste, mortar, and concrete and release this moisture during the hydration process. Autogenous shrinkage was first described 60 years ago by Mechtcherine [20]. During this process, when the volume of concrete decreased, its mass and temperature did not change considerably. However, because the autogenous shrinkage rate of normal concrete was smaller than its drying shrinkage rate, this problem had not been identified in high-performance concrete (HPC), which often exhibited autogenous shrinkage and cracking. Two methods have been generally used to inhibit the early cracking caused by self-desiccation and autogenous shrinkage. The first was to add a lightweight aggregate [21,22], and the second was to add SAPs [23]. This internal curing of SAPs aids in the curing process of concrete and allows SAPs to effectively regulate the level of moisture in concrete [10]. Although the addition of SAPs affects the mechanical properties of cement [24], environmental SEM results revealed that, after 28 days, the microstructures of SAP and SRA cement paste became saturated with micropores measuring 10-20 μm in size. This may explain the decreased compressive strength of SAP and SRA cement paste [25]. However, the addition of SAPs can reduce the autogenous and drying shrinkage of concrete [26–28]. Therefore, an alternative method is to use SAPs to achieve internal curing. Because SAPs involve a cross-link between acrylic acid and acrylamide and exhibit excellent chemical stability and high swelling performance in alkali brine concrete pore solutions, their applications in concrete have been confirmed to be successful [20,29]. SAPs can both absorb and store water, with an absorption capacity that reaches more than 30 times their own weight [30]. This process delays the reduction in internal humidity and reduces self-desiccation [31]. Wang [14] reported that SAPs reduced the autogenous shrinkage of HPC. In another study, Justs et al. [30] indicated that 28-day-old HPC exhibited a high shrinkage rate of 650 μm/m. However, after SAPs were added, this rate decreased to 150 μm/m [25] As an internal curing agent [23,32–34], SAPs are mainly used as the base material of cement. They effectively reduce the shrinkage of HPC in bridge floors [35] and high-strength mortar [36]. Several studies have indicated that internal curing is effective for the base materials of cement and alkaline-activated materials. Therefore, SAPs are considered internal curing agents that have the potential to reduce the self-desiccation and autogenous shrinkage of alkaline-activated blast furnace slag materials [37] Relevant studies have pointed out that the key drying shrinkage control time of the alkali-activated slag (AAS) is 7 days before the aging, and 50% of the total shrinkage of the AAS system mainly occurs. If the drying shrinkage can be slowed down, it can be quite helpful to the durability [38–41]. In this study, we used GGBFS as a base material to develop GGBFS geopolymers. Three types of polymer materials were used to obtain the geopolymer composites. The alkali equivalent, alkali modulus ratio, and liquid-to-solid ratio were set at 15%, 0.64, and 0.25, respectively. According to the above literature review, it is known that applications of geopolymers will be widely used in the civil engineering field in the future, but the problem of shrinkage still needs to be overcome. In this study, different SAP materials were used as the main material for slowing geopolymers. Through the high water absorption and small molecular characteristics of SAPs, the early drying shrinkage of geopolymers can be effectively slowed down so as to solve the urgent problem of geopolymer drying shrinkage.

2. Materials and Methods

2.1. Experiment Design

To develop GGBFS geopolymers, GGBFS was used as the base material, and the alkali activator in this test was a mixed solution of sodium hydroxide, sodium silicate, and water. The ratio from SiO_2 to Na_2O in the alkali activator affects the reaction and various properties in the inorganic polymer. The source of Na_2O is sodium hydroxide and sodium silicate; therefore, this test used an alkali equivalent and alkali modulus to control the ratio of SiO_2 and Na_2O in the alkali activator. The definitions of alkali equivalent and alkali modulus are as follows: Equations (1) and (2), where the alkali equivalent, alkali modulus

ratio, and liquid-to-solid ratio were set at 15%, 0.64, and 0.25. Three types of polymer materials were then added to the GGBFS geopolymers, and a gravimetric method was used to add 0.3%, 0.5%, 0.7%, and 0.9% polymer materials and obtain geopolymer composites. Finally, the specimens were demolded after 24 h and placed in the open air for curing.

$$Alkali\ equivalent = \frac{Na_2O}{Total\ Powder}(wt\%) \quad (1)$$

$$Alkali\ modulus\ ratio = \frac{SiO_2}{Na_2O}(Molar\ ratio) \quad (2)$$

2.2. Materials

2.2.1. GGBFS

The Blaine fineness (air permeability test) and specific gravity of GGBFS were 4207 cm^2/g and 2.93 g/cm^3, respectively, and this was provided by CHC Resources Corporation, Kaohsiung, Taiwan (see Figure 1); for the chemical composition analysis, see Table 1.

Figure 1. GGBFS.

Table 1. Chemical composition and physical properties of the raw materials.

Chemical Composition (%)		GGBFS	NaOH	Na_2SO_3 (wt%)
SiO_2		34.2		28
Al_2O_3		14.35		
Fe_2O_3		0.29	0.0004	<0.2
CaO		39.67		
MgO		7.75		
SO_3		0.57		
Na_2O		0.24		9
K_2O		0.28		
NaOH			98.2	
$NaCO_3$			0.165	
NaCL			0.0135	
Physical property	Fineness (cm^2/g)	4207	-	
	Specific gravity	2.93	0.598	1.38
	°Bé	-	-	37

2.2.2. PAM

PAM with a chemical formula of $[CH_2CH]_nCONH_2$, a specific gravity of 1.3, viscosity of 80–460 cps, and an average molecular weight of approximately 1.2 million atomic mass units (AMUs) was provided by Guan Heng Industrial, Taoyuan, Taiwan. Figure 2 shows

an SEM image of PAM. Notably, every 1 g of PAM can absorb approximately 250 g of water (distilled water).

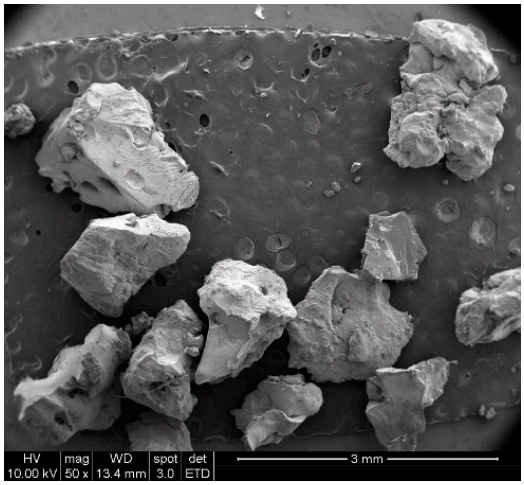

Figure 2. SEM image of PAM (50×).

2.2.3. SP

SP with a chemical formula of $CH_2CH(COONa)$, a specific gravity of approximately 1.2, a viscosity of approximately 5.25 cps, and an average molecular weight of approximately 1.2 million AMUs was provided by Guan Heng Industrial. Figure 3 shows an SEM image of SP. Notably, every 1 g of SP can absorb approximately 250 g of water (distilled water).

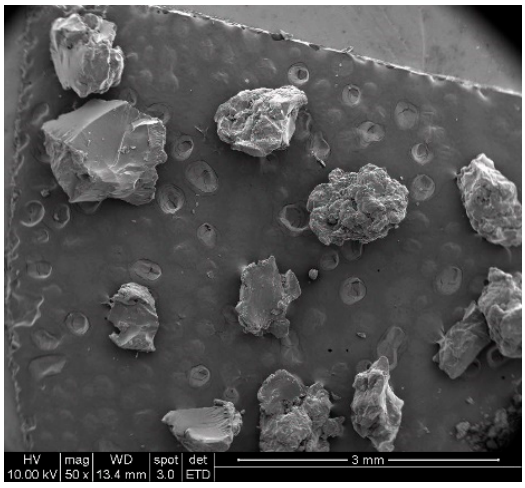

Figure 3. SEM image of SP (50×).

2.2.4. Sodium Tetraborate

Sodium tetraborate (ST) with a chemical formula of $Na_2B_4O_7{\cdot}10H_2O$, a specific gravity of approximately 1.73, and an average molecular weight of approximately 381 AMUs was provided by Guan Heng Industrial. Figure 4 shows an SEM image of ST. Notably, every 1 g of ST can absorb approximately 80–120 g of water (distilled water).

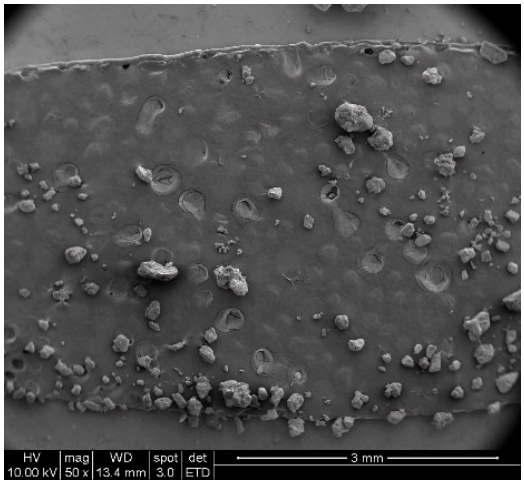

Figure 4. SEM image of ST (50×).

2.3. Experimental Variables and Ratios

As the drying shrinkage and thermal conductivity increase and weight loss decreases, the base equivalent also increases. To induce shrinkage, the alkali equivalent, alkali modulus ratio, and liquid-to-solid ratio were set at 15%, 0.64, and 0.25, respectively. The alkali activator mixture included sodium hydroxide, sodium metasilicate, and water. The ratios of SiO_2 and Na_2O in the alkali activator affected the reaction and performance of the geopolymers, and the Na_2O source contained sodium hydroxide and sodium metasilicate. Therefore, the alkali equivalent and alkali modulus ratio were used to control the ratios of SiO_2 and Na_2O in the alkali activator (see Table 2). Polymer materials were added to GGBFS geopolymers and cured in the open air for 3, 7, 14, 28, and 56 days under the following conditions: an alkali modulus ratio of 0.64, an alkali equivalent of 15%, a sodium hydroxide concentration of 10 M, and sodium metasilicate of 37° Be. The amount of polymer material added depended on the weight percentage of water-quenched GGBFS. The main variables were the type of polymer materials and the amount added. These variables are detailed as follows.

Amount of polymer material added: a gravimetric method was used to add 0.3%, 0.5%, 0.7%, and 0.9% polymer materials to GGBFS.

Types of polymer materials: PAM, SP, and ST were used.

Curing duration: the curing durations were 3, 7, 14, 28, and 56 days.

Table 2. Mixture proportions.

Mix Symbol	SP (g)	PAM (g)	ST (g)	GGBFS (g)	NaOH (g)	Na_2SiO_3 (g)	Water (g)
0.3 SP	0.3	-	-	100	14.66	32.26	8.57
0.5 SP	0.5	-	-				
0.7 SP	0.7	-	-				
0.9 SP	0.9	-	-				
0.3 PAM	-	0.3	-				
0.5 PAM	-	0.5	-				
0.7 PAM	-	0.7	-				
0.9 PAM	-	0.9	-				
0.3 ST	-	-	0.3				
0.5 ST	-	-	0.5				
0.7 ST	-	-	0.7				
0.9 ST	-	-	0.9				

SP: sodium polyacrylate; PAM: polyacrylamide; ST: sodium tetraborate; GGBFS: ground granulated blast furnace slag.

2.4. Experimental Setup

1. The length changes in GGBFS geopolymer specimens were measured according to ASTM C157 regulations [42]. The dimensions of the rectangular specimens were 285 mm × 25 mm × 25 mm, and the length change was measured every day at the ages of 1–14, 28, and 56 days:

$$\varepsilon = (L_2 - L_1) \div L_1 \times 100\%, \quad (3)$$

where ε is the change in length (%), L_1 is the initial length of the specimen after demolding (mm), and L_2 is the length measured at a specific age (mm).

2. Weight loss

Dehydrated sodium sulfate was used to prepare a saturated sodium sulfate solution according to ASTM C1012 [43]. The geopolymer specimens were soaked in the solution. After the GGBFS geopolymer specimens were obtained, they were aged for 7 and 28 days. Subsequently, they were placed in an oven for 24 h at 100 ± 5 °C and soaked in a saturated sodium sulfate solution for 24 h. This process was repeated five times to measure the weight loss ratio, which was calculated using the following equation:

$$(W_{end} - W_{begin}) \div W_{begin} \times 100\%, \quad (4)$$

where W_{begin} is the initial weight of the specimen (g), and W_{end} is the weight of the specimen after the test (g).

3. Steel ring strain (ring test)

As shown in Figure 5, the dimensions of the specimens were halved by the same ratio according to ASTM C1581 [44]. The materials were placed in two concentric steel rings; the inside diameter of the outer ring was 203 mm, and the outside diameter of the inner ring was 165 mm. The specimen was a hollow cylinder with a thickness of 19 mm and a height of 75 mm. Strain gauges were placed in four directions on the specimens to measure the strain.

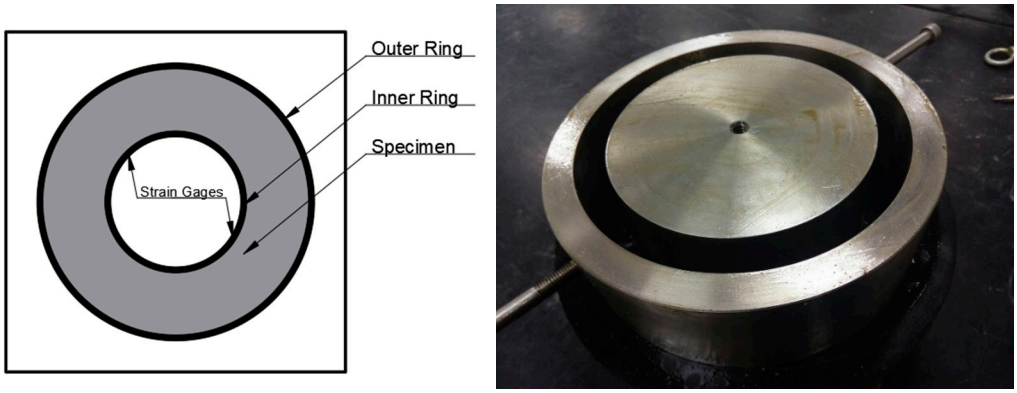

(**a**) (**b**)

Figure 5. Schematic of the ring test model. (**a**) Model required by ASTM C1581. (**b**) Schematic of a scaled-down model of ASTM C1581.

3. Results and Discussion

3.1. Length Change and Shrinkage of GGBFS Geopolymers

To investigate the durability of GGBFS geopolymers, we measured the length changes in the specimens to understand their degrees of shrinkage. As shown in Figure 6, the degree of shrinkage of the geopolymers depended on the type of polymer materials added. The results indicate that PAM exhibited the optimal shrinkage mitigation effect, followed by SP and ST. Folliard et al. [45,46] and Lura et al. [47] used polymer materials to reduce

the surface tension of pores, and their results indicated that the drying and autogenous shrinkage rates decreased [12,48].

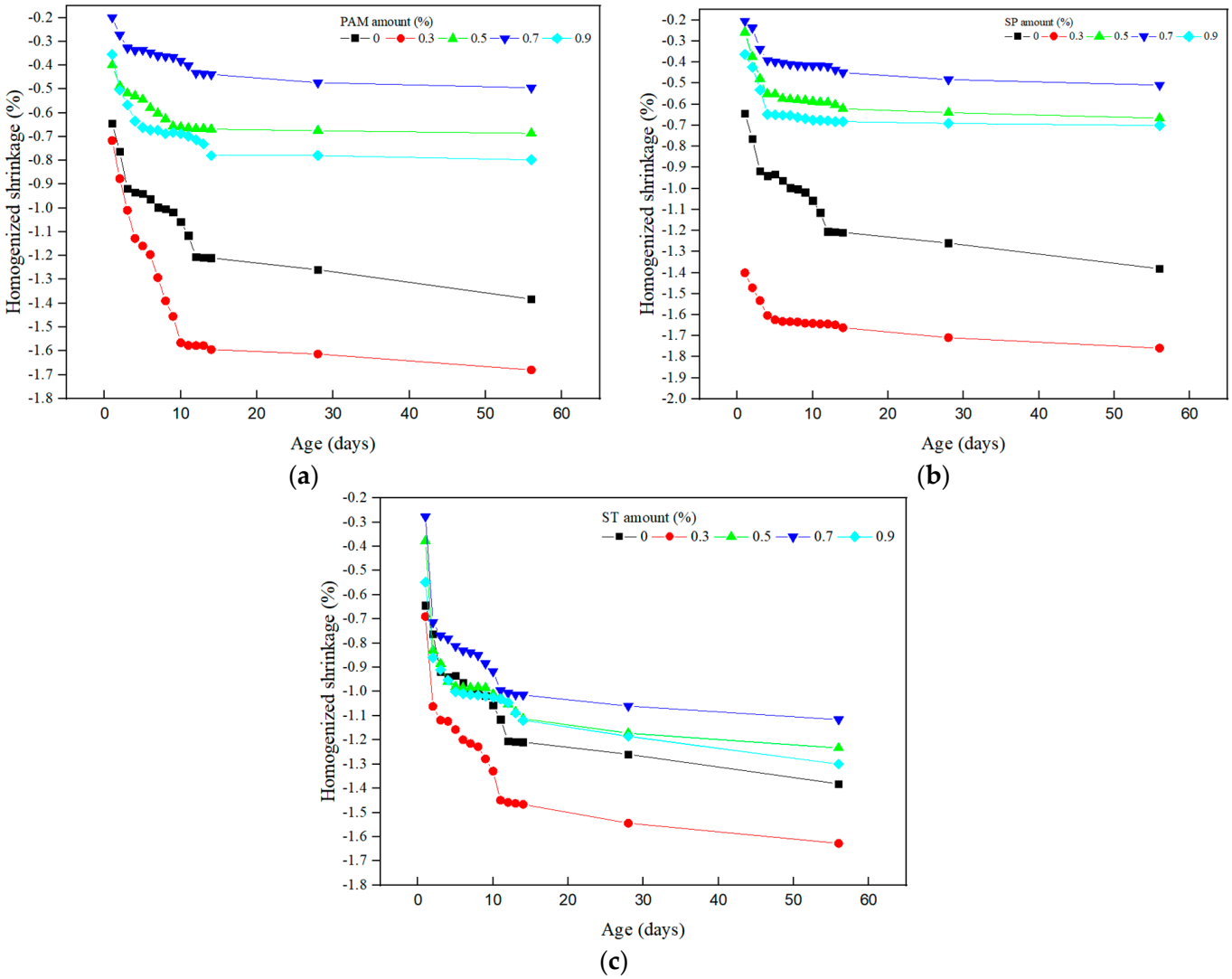

Figure 6. Drying shrinkage change after adding different SAPs. (**a**) Drying shrinkage for different additions of PAM. (**b**) Drying shrinkage for different additions of SP. (**c**) Drying shrinkage for different additions of ST.

As shown in Figure 6, when 0.3% PAM was added, the degree of shrinkage reached its highest value (−1.68%), whereas when 0.7% PAM was added, the degree of shrinkage reached its lowest value (−0.716%). Finally, when 0.3% and 0.7% SP were added, the degrees of shrinkage reached −1.759% and −0.509%, respectively, and the degree of shrinkage in the control group was −1.382%. Compared with the degree of shrinkage of the control group, the addition of 0.7% PAM decreased the degree of shrinkage by approximately 64%, whereas the addition of 0.3% PAM increased the degree of shrinkage by 21%. This is presumably because the addition of 0.3% polymer materials was insufficient. This finding accords with that of Song et al. [35], who reported that the concentration of polymer materials added should be 0.6% or higher. They also highlighted that the addition of only a small amount of polymer materials prevented the polymer material from incompletely absorbing moisture. Figure 6 shows the results obtained when ST was added. The optimal results were observed when 0.7% ST was added. However, the addition of 0.5% and 0.9% polymers materials to geopolymers composites at the age of 1–5 days resulted in a larger degree of shrinkage than in the control group. This is presumably because ST

released moisture slower than did PAM and SP. Therefore, it demonstrated a higher degree of shrinkage than that of the control group during the early stages.

As shown in Figure 7, the degree of shrinkage increased when 0.3%, 0.5%, 0.7%, and 0.9% polymer materials were added and aged for 1–3 days. Similarly, the degree of shrinkage for the control group also increased when they were aged for 1–3 days. However, although the GGBFS geopolymers exhibited early shrinkage, their degree of shrinkage decreased as they aged. When 0.3% of polymer materials were added, the degree of shrinkage exceeded that of the control group because this amount was insufficient. However, when 0.5%, 0.7%, and 0.9% PAM were added, optimal shrinkage mitigation results were observed. Compared with the degree of shrinkage for the control group, the degree of shrinkage decreased by 64% when 0.7% PAM was added.

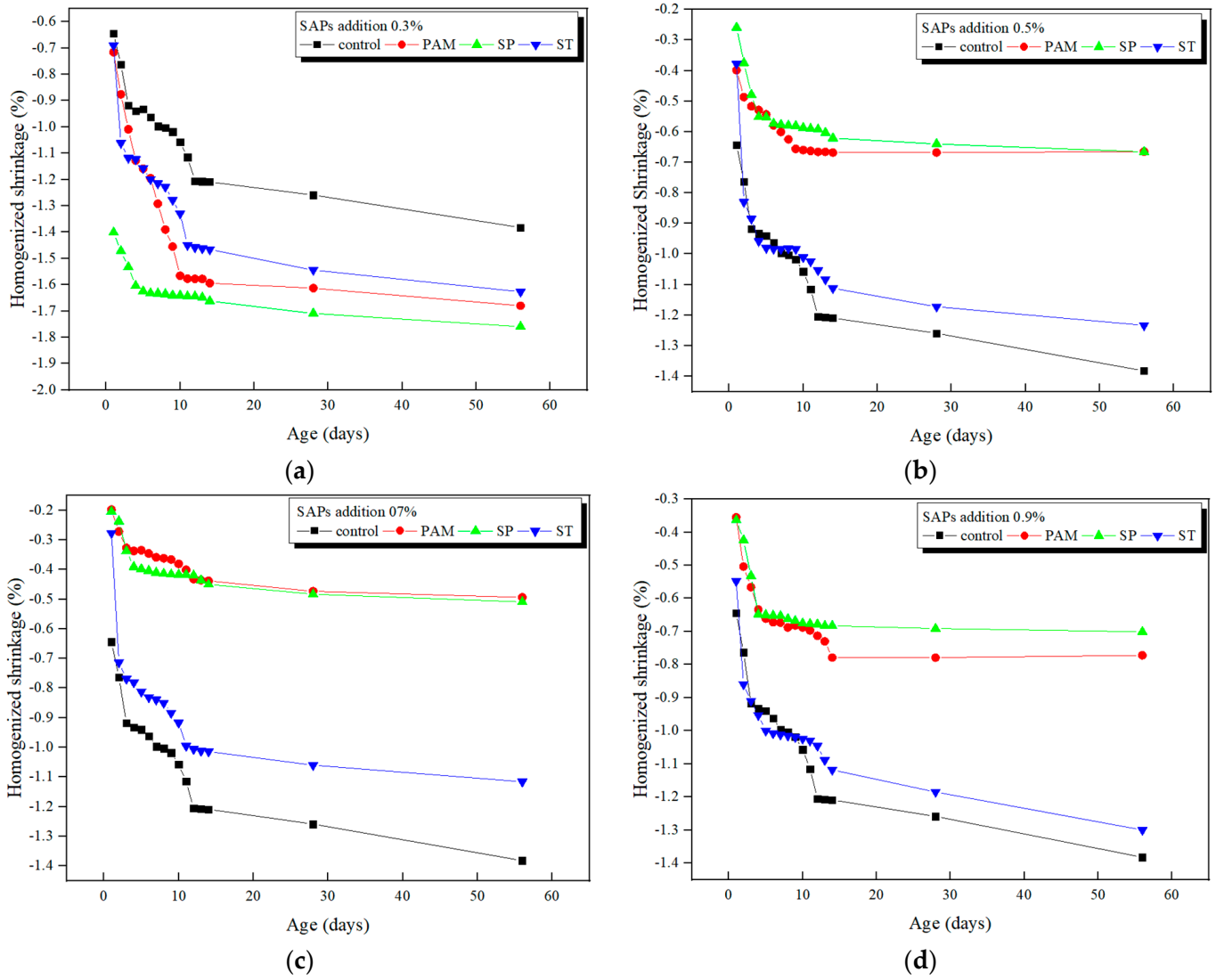

Figure 7. Comparison of drying shrinkage with different SAP contents added. (**a**) Changes in length from drying shrinkage when 0.3% of a given polymer material was added. (**b**) Changes in length from drying shrinkage when 0.5% of a given polymer material was added. (**c**) Changes in length from drying shrinkage when 0.7% of a given polymer was added. (**d**) Length changes from drying shrinkage when 0.9% polymer material was added.

3.2. Steel Ring Strain of GGBFS Geopolymers

The results of Section 3.1 in the length change (shrinkage) test indicated that the geopolymers exhibited higher degrees of shrinkage during the earlier stages. Geopolymer materials underwent 3 shrinkage deformations, all occurring 48 h after casting [48–50]. Therefore, during the restrained shrinkage test, the tensile stress characteristics of the mortar were used to measure the degree of shrinkage for GGBFS geopolymer composites at the age of 1–3 days. In accordance with the ASTM C1581 standard, strain gauges were placed in four directions on the specimens to measure the strain, and the dimensions of the specimens were halved by the same ratio. As shown in Figures 8–10, the GGBFS geopolymer composites started shrinking after 1 day. In addition, the strain resulted in several crests after 1 day because the specimen started to shrink, and cracks appeared on the surface.

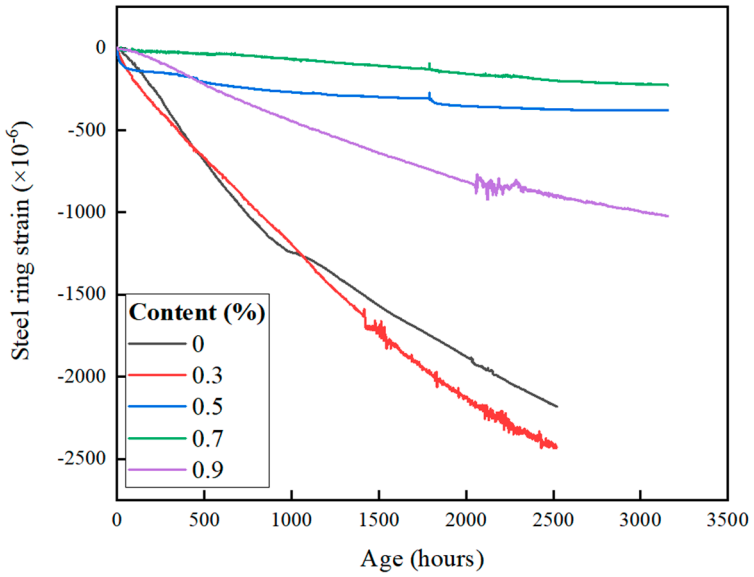

Figure 8. Steel ring strain of GGBFS geopolymers with PAM added.

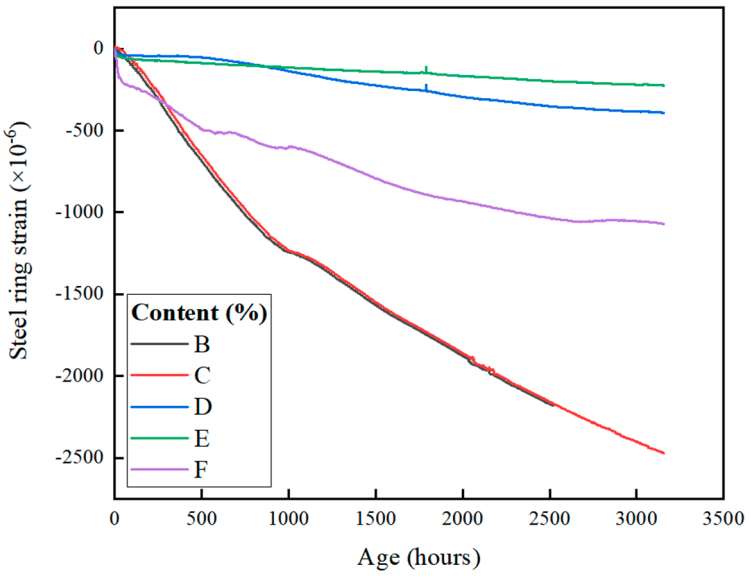

Figure 9. Steel ring strain of GGBFS geopolymers with SP added.

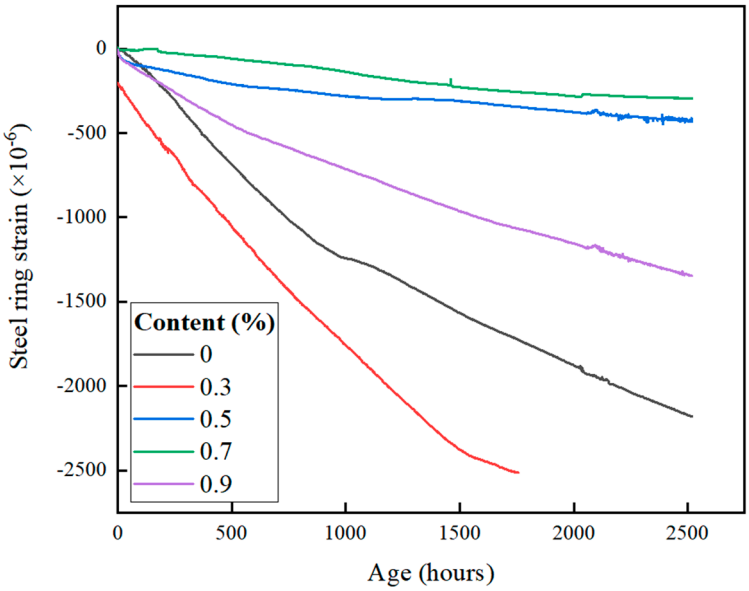

Figure 10. Steel ring strain of GGBFS geopolymers with ST added.

As shown in Figure 8, when 0.3%, 0.5%, 0.7%, and 0.9% PAM were added, the largest strains observed were 2436×10^{-6}, 380.3×10^{-6}, 225×10^{-6}, and 1025×10^{-6}, respectively. The strain of the control group was 2182×10^{-6}. As indicated by the strain curve, when 0.3% PAM was added, several crests were observed after 0.9 days. This is presumably because tiny cracks started developing on the surface. The addition of 0.7% or 0.5% PAM resulted in surface cracks after 1.2 days, whereas surface cracks were observed in the control group after 0.1 days. As shown in Figure 9, when 0.7% SP was added, the largest strain was also 225×10^{-6}, which is the same as when 0.7% PAM was added. Because PAM and SP had a similar water absorption rate, their largest strains were similar. When 0.3% ST was added, surface cracks appeared after 1 day, as depicted in Figure 10. However, compared with PAM and SP, when ST was added, surface cracks were observed 0.8-1.3 days earlier. In addition, because ST had a lower water absorption rate than that of PAM and SP, moisture was rapidly lost, resulting in increased strain and surface cracks. Hence, among the three polymer materials, ST exhibited the worst performance.

The addition of 0.7% polymer materials decreased the degree of shrinkage of the GGBFS geopolymers. This is presumably because shrinkage is a result of exothermic dehydration. After a specimen reaches a certain degree of shrinkage, cracks start to develop. Adding a polymer material helps absorb the moisture and slowly release it, thereby effectively mitigating the loss of moisture and slowing down the process of shrinkage and cracking [51–55] Although the addition of SAPs can effectively slow down drying shrinkage, when added at 0.9%, it can also cause more voids inside the test body due to the moisture released by the SAPs, resulting in an addition of 0.9%. As a result, the drying shrinkage effect is reduced.

3.3. Weight Loss of GGBFS Geopolymers under Sulfate Acid Attacks

Sulfate-containing environments affect the durability of structures and induce cracks and damage. In this study, we conducted experiments according to ASTM C1012 [43] GGBFS geopolymer specimens, which were cured for 7 and 28 days. The specimens were then soaked in a saturated sulfate solution, and the process was repeated five times. Weight loss was measured at regular intervals to determine the soundness of the specimens, and the results are presented in Figures 11 and 12.

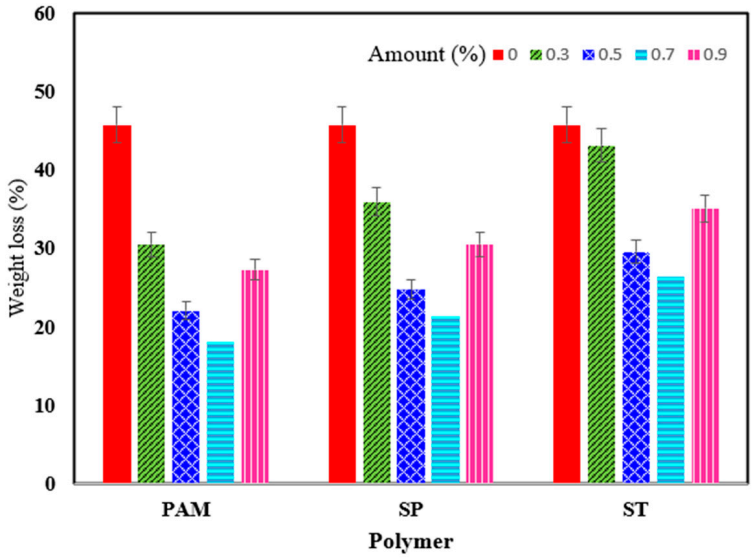

Figure 11. Weight loss of GGBFS geopolymers under sulfate acid attacks at 7 days.

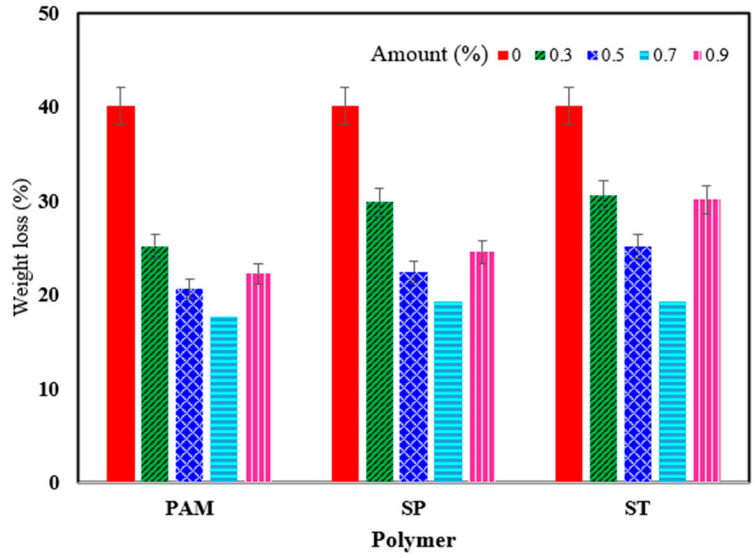

Figure 12. Weight loss of GGBFS geopolymers under sulfate acid attacks at 28 days.

The weight losses of GGBFS geopolymers at an age of 7 days after 5 cycles of sulfate attacks are presented in Figure 11. The weight loss of PAM was between 18.11% and 30.53%, the weight loss of SP was between 21.31% and 35.89%, and the weight loss of ST was between 23.34% and 40.09%; by comparison, the weight loss of the control group was 45.71%. Among the three polymer materials, PAM exhibited the smallest weight loss because the degree of shrinkage associated with PAM resulted in cracks and specimen breakdown.

The weight loss of the polymer materials at an age of 28 days is presented in Figure 12 The weight loss of PAM was between 17.61% and 25.13%, the weight loss of SP was between 19.31% and 29.85%, and the weight loss of ST was between 19.3% and 30.55%, whereas the weight loss of the control group was 40.09%. The test results indicated that the 28-day-old polymer materials were more resistant to sulfate attacks than the 7-day-old polymer materials. In addition, because the specimens were more developed, they exhibited superior durability against sulfate attacks.

3.4. GGBFS Geopolymers Crack Propagation Imaging

In general, crack propagation develops when a specimen reaches a certain degree of shrinkage. As indicated by the test results, the GGBFS geopolymer composites exhibited a higher degree of shrinkage during the earlier stages. If the drying shrinkage of geopolymers could be effectively monitored through general imaging technology, there would be considerable changes in the application of civil materials in the future. Therefore, we used image processing to monitor the surface crack propagation changes in samples aged 0–3 days, recording the crack opening time and calculating the crack propagation area ratio of the plane to understand the slowing crack status of SAP. We regarded the test body area of the image to be 100% when measuring the length and width of the resulting cracks, calculating them as areas, and comparing the crack drying shrinkage changes in 3 different SAP materials. The ratios of the areas occupied by the crack propagation were calculated, and the results are presented in Figure 13. The red, blue, green, and black lines represent the crack propagation generated after 6 h, 1 day, 2 days, and 3 days, respectively. The results indicate that the control group developed cracks 6 h after the specimens were filled with paste, whereas the specimens with polymer materials developed cracks 1 day after they were filled with paste. A comparison of the three types of polymer materials indicates that when PAM, SP, and ST were added, the damaged areas of the specimens were approximately 0.2%, 0.27%, and 0.35%, respectively, of the total area, whereas the damaged area of the control group represented 0.67% of the total area. The addition of the polymer materials reduced the degree of shrinkage by approximately 40%. These polymer materials effectively decreased the degree of shrinkage because they absorbed and stored water. After the GGBFS geopolymers were produced, the polymer materials slowly released their stored moisture and reduced the degree of shrinkage. Although the reaction mechanism and chemical results of geopolymers are different from those of cement systems, they can still slow down their dry shrinkage state [56,57]. To clearly understand the mechanism underlying pore fractures, we conducted several optical microscopy (OM) experiments. The results are presented in Figure 14. Using binarization, we analyzed the size of the crack propagation. Through the imaging technology of OM, the crack propagation under the same area was analyzed. The cracks of the control organization accounted for 0.17% of the overall area, the cracks of PAM accounted for 0.66% of the overall area, the cracks of SP accounted for 0.68% of the overall area, and the ST crack area accounted for 0.86% of the overall area. The formation of cracks usually affects compressive strength. Wu et al. [58] added polymer materials to high-performance cement composites. They reported that these polymer materials slowed down the drying shrinkage process of cement-based materials but increased the number of cracks and affected the compressive strength.

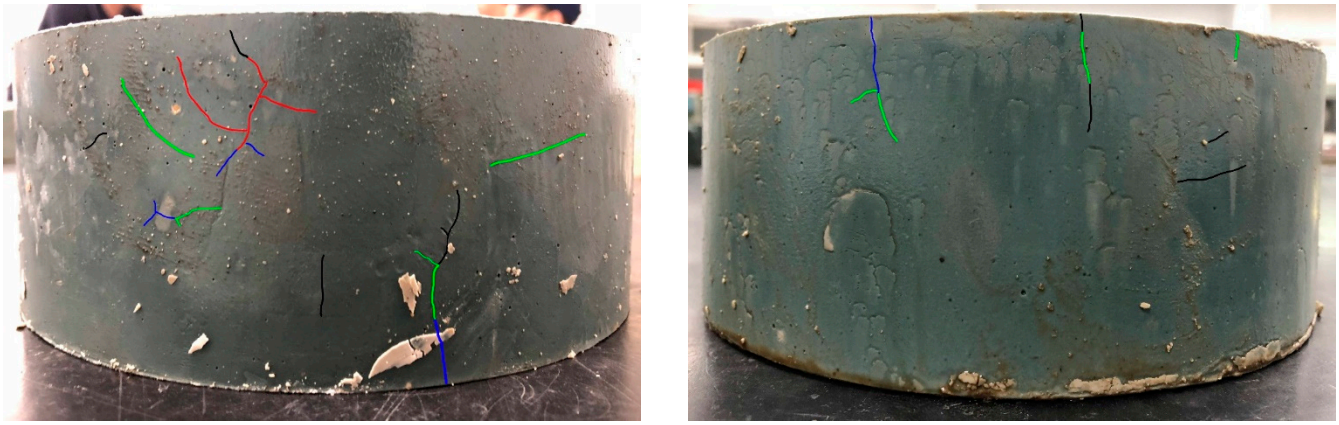

(**a**) (**b**)

Figure 13. *Cont.*

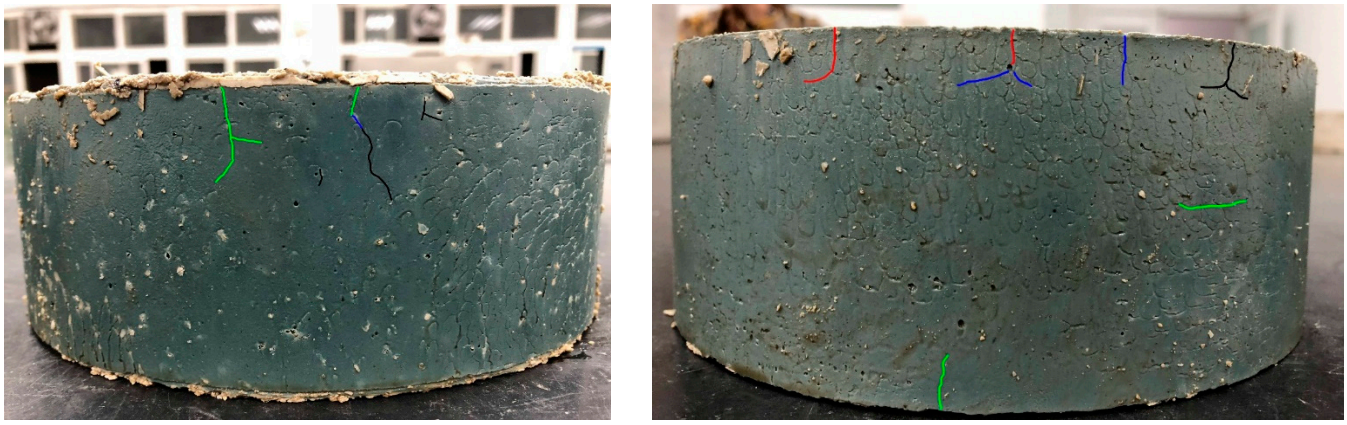

(**c**) (**d**)

Figure 13. Effects of different polymer materials on the cracking behavior of GGBFS geopolymers. (**a**) Crack development in the control group. (**b**) Crack development with 0.7% PAM added. (**c**) Crack development with 0.7% SP added. (**d**) Crack development with 0.7% ST added. (The red, blue, green, and black lines represent the crack propagation generated after 6 h, 1 day, 2 days, and 3 days).

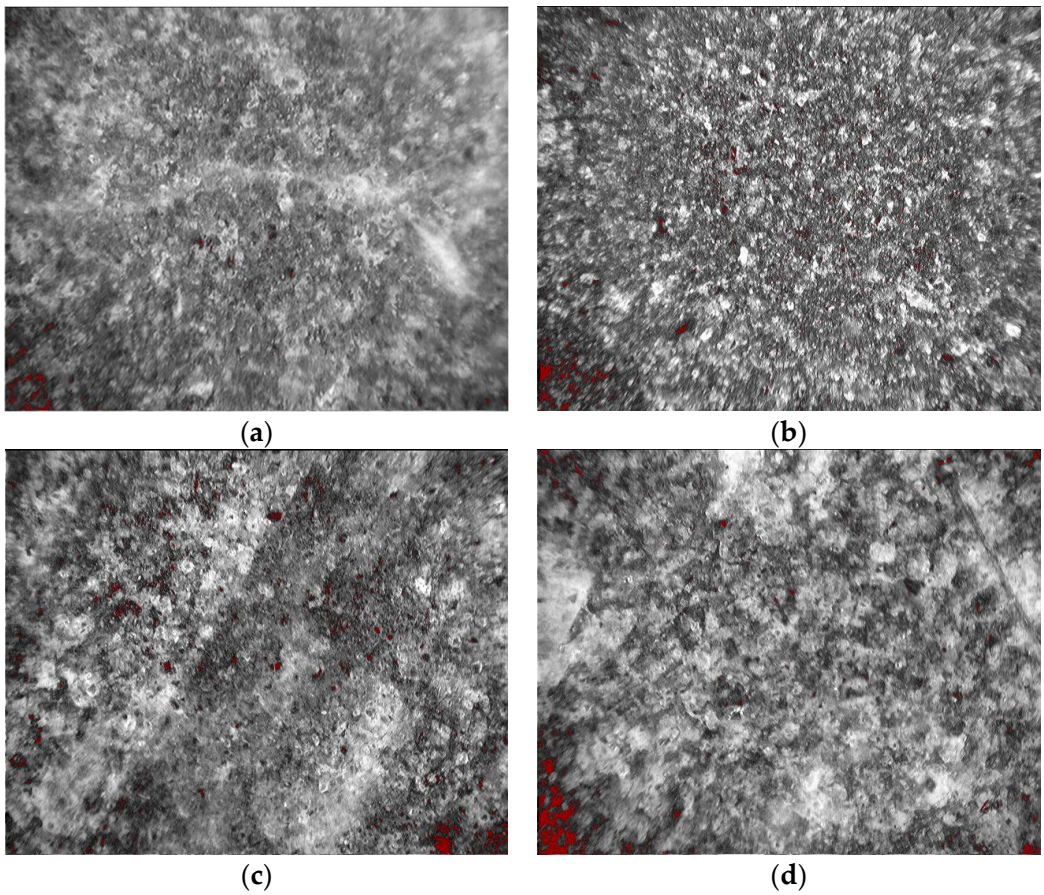

(**a**) (**b**)

(**c**) (**d**)

Figure 14. OM images of porosity distribution for different polymer materials. (**a**) OM image of porosity distribution in the control group. (**b**) OM image of porosity distribution with 0.7% PAM. (**c**) OM image of porosity distribution with 0.7% SP. (**d**) OM image of porosity distribution with 0.7% ST.

4. Conclusions

1. The homogenized shrinkage results indicated that the addition of 0.7% polymer materials mitigated shrinkage the best. The length changes in PAM, SP, and ST at an age of 56 days were 64%, 63%, and 19%, respectively.
2. The ring test results indicate that the total strain of the control group at an age of 3 days was 2182×10^{-6}. After 0.7% PAM was added, the total strain reached 225×10^{-6}; that is, the degree of shrinkage decreased by 89%, which is the largest decrease noted in this study.
3. Cracks appeared when a specimen sustained a certain amount of shrinkage. The larger the number of cracks, the lower the durability of the specimen against sulfate attacks. Therefore, when the degree of shrinkage decreased, the number of cracks also decreased. In this study, the addition of 0.7% PAM resulted in optimal durability against sulfate attacks, with a weight loss of approximately 17.61%.
4. The image analysis results indicate that the addition of polymer materials effectively reduced the degree of shrinkage of GGBFS geopolymers.

Author Contributions: Conceptualization, W.-T.K. and Y.-W.S.; Data curation, C.-U.J. and Y.-W.S.; Formal analysis, W.-T.K. and C.-U.J.; Investigation, W.-T.K.; Methodology, W.-T.K. and Y.-W.S.; Project administration, W.-T.K.; Resources, W.-T.K. and Y.-W.S.; Supervision, W.-T.K.; Validation, W.-T.K. and C.-U.J.; Visualization, Y.-W.S.; Writing—review and editing, W.-T.K. and C.-U.J. All authors have read and agreed to the published version of the manuscript.

Funding: This research was funded by National Science and Technology Council, grant number: MOST 111-2637-E-992-002.

Data Availability Statement: The study did not report any data availability statement; all data were sourced from real experiments.

Conflicts of Interest: The authors declare no conflict of interest.

References

1. You, N.Q.; Li, B.L.; Cao, R.L.; Shi, J.J.; Chen, C.; Zhang, Y.M. The influence of steel slag and ferronickel slag on the properties of alkali-activated slag mortar. *Constr. Build. Mater.* **2019**, *227*, 116614. [CrossRef]
2. Adediran, A.; Yliniemi, J.; Moukannaa, S.; Ramteke, D.D.; Perumal, P.; Illikainen, M. Enhancing the thermal stability of alkali-activated Fe-rich fayalite slag-based mortars by incorporating ladle and blast furnace slags: Physical, mechanical and structural changes. *Cem. Concr. Res.* **2023**, *166*, 107098. [CrossRef]
3. Konstantinos, K.; Georgios, B.; Vasiliki, K.; Evangelos, P.; Witold, K.; Grzegorz, P.; Jarosław, K. Assessment of Alkali Activation Potential of a Polish Ferronickel Slag. *Sustainability* **2019**, *11*, 1863. [CrossRef]
4. Konstantinos, K.; Lourdes, Y.; Georgios, B.; Vasiliki, K.; Evangelos, P. Factors affecting co-valorization of fayalitic and ferronickel slags for the production of alkali activated materials. *Sci. Total Environ.* **2020**, *721*, 137753. [CrossRef]
5. Lin, B.Z. *A Study on Testing Mortar Properties with a Cement Replacement by Using Reducing Slag*; National Taipei University of Technology Department of Civil Engineering: Taipei, Taiwan, 2012.
6. Komnitsas, K.A. Potential of geopolymer technology towards green buildings and sustainable cities. *Procedia Eng.* **2011**, *21*, 1023–1032. [CrossRef]
7. Wang, S.D.; Pu, X.C.; Scrivener, K.L.; Pratt, P.L. No Access Alkali-activated slag cement and concrete: A review of properties and problems. *Advances in, Cem. Concr. Res.* **1995**, *7*, 93–102. [CrossRef]
8. Yang, L.C.; Cheng, T.W. Effects of fillers on improving shrinkage of inorganic polymers made from ground granulated blast furnace slag. *Min. Metall. Dep. Taipei Inst. Technol.-Taiwan Univ. Sci. Technol. Educ. Found. J.* **2011**, *5*, 48–53.
9. Olawuyi, B.J.; Boshoff, W.P. Influence of SAP content and curing age on air void distribution of high performance concrete using 3D volume analysis. *Constr. Build. Mater.* **2017**, *135*, 580–589. [CrossRef]
10. Ma, X.; Liu, J.; Wu, Z.; Shi, C. Effects of SAP on the properties and pore structure of high performance cement-based materials. *Constr. Build. Mater.* **2017**, *131*, 476–484. [CrossRef]
11. Plank, J.; Sakai, E.; Miao, C.; Yu, C.; Hong, J. Chemical admixtures-Chemistry, applications and their impact on concrete microstructure and durability. *Cem. Concr. Res.* **2015**, *78*, 81–99. [CrossRef]
12. Yang, Z.X.; Shi, P.; Zhang, Y.; Li, Z.M. Effect of superabsorbent polymer introduction on properties of alkali-activated slag mortar. *Constr. Build. Mater.* **2022**, *340*, 127541. [CrossRef]
13. Tu, W.L.; Zhu, Y.; Fang, G.H.; Wang, X.G.; Zhang, M.Z. Internal curing of alkali-activated fly ash-slag pastes using superabsorbent polymer. *Cem. Concr. Res.* **2019**, *116*, 179–190. [CrossRef]

14. Wang, J.H.; Cheng, T.W. *Study on Shrinkage Properties and Durability of Inorganic Polymer Green Cement and Concrete*; The Chinese Institute of Environmental Engineering: Kaohsiung, Taiwan, 2015; pp. 1–12.
15. Bakharev, T.; Sanjayan, J.G.; Cheng, Y.B. Effect of admixtures on properties of alkali-activated slag concrete. *Cem. Concr. Res.* **2000**, *30*, 1367–1374. [CrossRef]
16. Palacios, M.; Puertas, F. Effect of shrinkage-reducing admixtures on the properties of alkali—Activated slag mortars and pastes. *Cem. Concr. Res.* **2007**, *37*, 691–702. [CrossRef]
17. Bakharev, T.; Sanjayan, J.G.; Cheng, Y.B. Effect of Elevated temperature curing on properties of alkali-activated slag concrete. *Cem. Concr. Res.* **1999**, *29*, 1619–1625. [CrossRef]
18. Jin, M.L.; Zhong, W.O.; Jin, C.M.; Ya, H.W.; Wu, H. The effect of SCMs and SAP on the autogenous shrinkage and hydration process of RPC. *Constr. Build. Mater.* **2017**, *155*, 239–249.
19. *NO.16*; JSCE Standard Specifications for Design and Construction of Concrete Structures. JSCE: Tokyo, Japan, 2007.
20. Schröfl, C.; Mechtcherine, V.; Gorges, M. Relation between the molecular structure and the efficiency of superabsorbent polymers (SAP) as concrete admixture to mitigate autogenous shrinkage. *Cem. Concr. Res.* **2012**, *42*, 865–873. [CrossRef]
21. Weber, S.; Reinhardt, H.W. A new generation of high performance concrete: Concrete with autogenous curing. *Adv. Cem. Based Mater.* **1997**, *6*, 59–68. [CrossRef]
22. Bentz, D.P.; Snyder, K.A. Protected paste volume in concrete: Extension to internal curing using saturated lightweight fine aggregate. *Cem. Concr. Res.* **1999**, *29*, 1863–1867. [CrossRef]
23. Jensen, O.M.; Hansen, P.F. Water-entrained cement-based materials-I: Principle and theoretical background. *Cem. Concr. Res.* **2001**, *31*, 647–654. [CrossRef]
24. Ma, X.W.; Zhang, J.K.; Liu, J.H. Review on superabsorbent polymer as internal curing agent of high performance cement-based material. *J. Chin. Chem. Soc. China* **2015**, *43*, 1099–1110.
25. Zheng, X.G.; Han, M.; Liu, L.L. Effect of Superabsorbent Polymer on the Mechanical Performance and Microstructure of Concrete. *Materials* **2021**, *14*, 3232. [CrossRef]
26. Hasholt, M.T.; Jensen, O.M.; Kovler, K.; Zhutovsky, S. Can superabsorent polymers mitigate autogenous shrinkage of internally cured concrete without compromising the strength? *Constr. Build. Mater.* **2012**, *31*, 226–230. [CrossRef]
27. Chen, X.P.; Shan, G.R.; Huang, J.; Huang, Z.M.; Weng, Z.X. Synthesis and properties of acrylic-based superabsorbent. *J. Appl. Polym. Sci.* **2004**, *92*, 619–624. [CrossRef]
28. Esteves, L.P.; Cachim, P.; Ferreira, V.M. Mechanical properties of cement morats with superabsorbent polymers. In *Advances in Construction Materials*; Springer: Berlin/Heidelberg, Germany, 2007; pp. 451–462.
29. Shen, D.J.; Wang, T.; Chen, Y.; Wang, M.L.; Jiang, G.Q. Effect of internal curing with super absorbent polymers on the relative humidity of early-age concrete. *Constr. Build. Mater.* **2015**, *99*, 246–253. [CrossRef]
30. Justs, J.; Wyrzykowski, M.; Bajare, D.; Lura, P. Internal curing by superabsorbent polymers in ultra-high performance concrete. *Cem. Concr. Res.* **2015**, *76*, 82–90. [CrossRef]
31. Mo, J.; Ou, Z.; Zhao, X.; Liu, J.; Wang, Y. Influence of superabsorbent polymer on shrinkage properties of reactive powder concrete blended with granulated blast furnace slag. *Constr. Build. Mater.* **2017**, *146*, 283–296. [CrossRef]
32. Mechtcherine, V.; Reinhardt, H. *Application of Super Absorbent Polymers (SAP) in Concrete Construction State of the Art Reports Prepared by Technical Committee 225-SAP*; Springer: Berlin/Heidelberg, Germany, 2012.
33. Snoeck, D.; Jensen, O.M.; De Belie, N. The influence of superabsorbent polymers on the autogenous shrinkage properties of cement pastes with supplementary cementitious materials. *Cem. Concr. Res.* **2015**, *74*, 59–67. [CrossRef]
34. Craeye, B.; Geirnaert, M.; De Schutter, G. Super absorbing polymers as an internal curing agent for mitigation of early-age cracking of high-performance concrete bridge decks. *Constr. Build. Mater.* **2011**, *25*, 1–13. [CrossRef]
35. Mousavi, S.S.; Ouellet-Plamondon, C.M.; Guizani, L.; Bhojaraju, C.; Brial, V. On mitigating rebar-concrete interface damages due to the pre-cracking phenomena using superabsorbent polymers. *Constr. Build. Mater.* **2020**, *253*, 119181. [CrossRef]
36. Ribeiro, A.B.; Vinagre, M.; Goncalves, A. Shrinkage of mortars with a suspension of superabsorbent polymers. In Proceedings of the International RILEM Conference on Use of Superabsorbent Polymers and Other New Additives in Concrete, Lyngby, Denmark, 15–18 August 2010; RILEM Publications SARL: Bagneux, France, 2010.
37. Song, C.; Choi, Y.C.; Choi, S. Effect of internal curing by superabsorbent polymers—Internal relative humidity and autogenous shrinkage of alkali-activated slag mortars. *Constr. Build. Mater.* **2016**, *123*, 198–206. [CrossRef]
38. Al Makhadmeh, W.; Soliman, A. Understanding the shrinkage behaviour of alkali-activated slag binders modified by the superabsorbent polymer. *Constr. Build. Mater.* **2023**, *365*, 130053. [CrossRef]
39. Thomas, R.J.; Lezama, D.; Peethamparan, S. On drying shrinkage in alkali-activated concrete: Improving dimensional stability by aging or heat-curing. *Cem. Concr. Res.* **2017**, *97*, 13–23. [CrossRef]
40. Al Makhadmeh, W.A.; Soliman, A. Effect of activator nature on property development of alkali-activated slag binders. *J. Sustain. Cem. Based Mater.* **2020**, *10*, 240–256. [CrossRef]
41. Chen, W.W.; Li, B.; Wang, J.; Thom, N.C. Effects of alkali dosage and silicate modulus on autogenous shrinkage of alkali-activated slag cement paste. *Cem. Concr. Res.* **2021**, *141*, 106322. [CrossRef]
42. *ASTM C157*; Standard Test Method for Length Change of Hardened Hydraulic-Cement Mortar and Concrete. ASTM Standards: West Conshohocken, PA, USA, 2014.

43. *ACTM C1012*; Standard Test Method for Length Change of Hydraulic-Cement Mortars Exposed to a Sulfate Solution. ASTM Standards: West Conshohocken, PA, USA, 2004.
44. *ASTM C1581*; Standard Test Method for Determining Age at Cracking and Induced Tensile Stress Characteristics of Mortar and Concrete under Restrained Shrinkage. ASTM Standards: West Conshohocken, PA, USA, 2018.
45. Collepardi, M.; Borsoi, A.; Collepardi, S.; Olagot, J.J.O.; Troli, R. Effects of shrinkage reducing admixture in shrinkage compensating concrete under non-wet curing conditions. *Cem. Concr. Compos.* **2005**, *27*, 704–708. [CrossRef]
46. Folliard, K.J.; Berke, N.S. Properties of high-performance concrete containing shrinkage-reducing admixture. *Cem. Concr. Res.* **1997**, *27*, 1357–1364. [CrossRef]
47. Lura, P.; Jensen, O.M.; van Breugel, K. Autogenous shrinkage in high-performance cement paste: An evaluation of basic mechanisms. *Cem. Concr. Res.* **2003**, *33*, 223–232. [CrossRef]
48. Xie, T.; Fang, C.; Mohamad, M.S.; Visintin, A.P. Characterizations of autogenous and drying shrinkage of ultra-high performance concrete (UHPC): An experimental study. *Cem. Concr. Compos.* **2018**, *91*, 156–173. [CrossRef]
49. Li, Z.; Nedeljković, M.; Chen, B.; Ye, G. Mitigating the autogenous shrinkage of alkali-activated slag by metakaolin. *Cem. Concr. Res.* **2019**, *122*, 30–41. [CrossRef]
50. Li, Z.; Ye, G. Experimental study of the chemical deformation of metakaolin based geopolymer. In Proceedings of the SynerCrete, Funchal, Portugal, 24–26 October 2018; p. 18.
51. Potapova, E.N.; Manushina, A.S.; Urbanov, A.V. Effect of kaolin heat treatment on its properties1. *Refract. Ind. Ceram.* **2018**, *58*, 525–529. [CrossRef]
52. Jiang, D.; Li, X.; Lv, Y.; Li, C.; Jiang, W.; Liu, Z.; Xu, J.; Zhou, Y.; Dan, J. Autogenous shrinkage and hydration property of alkali activated slag pastes containing superabsorbent polymer. *Cem. Concr. Res.* **2021**, *149*, 106581. [CrossRef]
53. Li, Z.; Zhang, S.; Liang, X.; Granja, J.; Azenha, M.; Ye, G. Internal curing of alkali-activated slag-fly ash paste with superabsorbent polymers. *Constr. Build. Mater.* **2020**, *263*, 1200985. [CrossRef]
54. Li, Z.; Wyrzykowski, M.; Dong, H.; Granja, J.; Azenha, M.; Lura, P.; Ye, G. Internal curing by superabsorbent polymers in alkali-activated slag. *Cem. Concr. Res.* **2020**, *135*, 106123. [CrossRef]
55. Vafaei, B.; Farzanian, K.; Ghahremaninezhad, A. The influence of superabsorbent polymer on the properties of alkali-activated slag pastes. *Constr. Build. Mater.* **2020**, *236*, 117525. [CrossRef]
56. Oh, S.; Choi, Y.C. Superabsorbent polymers as internal curing agents in alkali activated slag mortars. *Constr. Build. Mater.* **2018**, *159*, 1–8. [CrossRef]
57. Yang, J.B.; Sun, Z.P.; Belie, N.D.; Snoeck, D.D. Mitigating plastic shrinkage cracking in alkali-activated slag systems by internal curing with superabsorbent polymers. *Cem. Concr. Compos.* **2022**, *134*, 104784. [CrossRef]
58. Wu, L.S.; Yu, Z.H.; Zhang, C.; Yuan, Z.; Bangi, T.Y. Shrinkage and tensile properties of ultra-high-performance engineered cementitious composites (UHP-ECC) containing superabsorbent polymers (SAP) and united expansion agent (UEA). *Constr. Build. Mater.* **2022**, *339*, 127697. [CrossRef]